Cryolite overcoated aluminum reflectors for far-ultraviolet spectroscopy

Javier Del Hoyo[a], Luis Rodriguez de-Marcos[b], J. Hennessy[c], M. Batkis[a], C. Bos[a], and Manuel Quijada[a]
[a]NASA Goddard Space Flight Center
[b]The Catholic University of America
[c]Jet Propulsion Laboratory, California Institute of Technology

ABSTRACT

Aluminum (Al) mirrors are conventionally protected with metal-fluoride coatings (e.g., MgF_2, LiF, or AlF_3) immediately after deposition to prevent oxidation and preserve its far-ultraviolet (FUV) spectral efficiency. However, the resulting FUV reflectance of the aluminum reflector is limited by the metal-fluoride overcoat film index of refraction, morphology, stoichiometry, and its absorption cut-off in the lower end of the FUV spectra. Cryolite (sodium hexafluoroaluminate, Na_3AlF_6) emerges as a potential candidate to preserve the aluminum FUV reflectance due to its relatively lower index of refraction in the visible to ultraviolet; therefore, allowing for the thin-film design of highly spectral efficient reflectors over a wide spectral range. We investigate the use of cryolite in aluminum reflector FUV coating design. The deposited aluminum reflector overcoated with cryolite will be examined in terms of spectral efficiency and environmental durability. The deposited cryolite overcoat will be evaluated in terms of optical constants and structural properties. Preliminary results have shown that the use of cryolite as an overcoat to protect aluminum would yield unprecedented results as an optimal Hydrogen Lyman-alpha (HLyα) spectral line reflector, with experimental reflectance values >96%.

Keywords: cryolite, reactive physical vapor deposition, rPVD, ultraviolet, UV, far-ultraviolet, FUV, sodium hexafluoroaluminate Na_3AlF_6

1. INTRODUCTION

For decades, the aluminum (Al) coating with a magnesium fluoride (MgF_2) overcoat protection layer has been the primary coating utilized for astrophysics ion transition-temperature gas analysis due to its high spectral efficiency over the FUV spectral range, greater relative environmental durability compared to other metal-fluoride overcoats on aluminum, and flight heritage [1,2]. As Al requires an overcoat to serve as a hermetic barrier and protect it from oxidation before exposed to atmospheric conditions, there have been various efforts to optimize this MgF_2 overcoat layer and increase its FUV spectral efficiency by heating during or after the deposition process to increase its respective packing density, depositing at high deposition rates, and utilizing atomic layer deposition (ALD) to grow the material [1,3,4]. Ultimately, the highest performing coatings have shown a peak reflectance of ~91% at the HLyα line of hydrogen (121.6 nm) with the longer wavelength end of FUV spectral range decreasing to ~80% at 160 nm [1,3].

We demonstrate cryolite as a replacement for MgF_2 to be used as the protective overcoat layer in FUV reflector design for applications at wavelengths >120 nm. Cryolite has highly desirable optical properties as its low index of refraction in the visible to infrared allow it to be used in various multilayer coating and bandpass filter designs [5-9]. Its large index contrast relative to higher index dielectric materials allow it to be paired in bandpass filter designs achieving spectral efficiencies of >99% in the visible to infrared spectral range [5-8]. In this manuscript, we study the spectral, surface, and environmental durability properties of the cryolite overcoat over Al coating. We will present spectral reflectance data from the far-ultraviolet to the infrared, optical dispersion constants of the cryolite material, surface roughness, and property changes of the film after aging.

2. COATING DEPOSITION AND CHARACTERIZATION PROCESSES

2.1 Optical thin film coating deposition processes

The Al/cryolite coating was deposited on pre-cleaned soda-lime glass substrates using resistive thermal evaporation, a physical vapor deposition (PVD) process. The coatings chamber was evacuated using a two-stage vacuum pump system consisting of a rotary vane pump and cryogenic pump reaching base pressures of $1.0x10^{-8}$ for all coating process. High-purity aluminum was evaporated from tungsten filaments following with the deposition of 99.5% pure cryolite. A quartz crystal in-situ film thickness monitor was used to monitor respective rates and final deposited thickness of the Al and cryolite films. Nominal deposition rates of 13.8-16.0 nm/sec and ~5 nm/sec were observed for each respective Al and cryolite material.

2.2 Enhancing environmental hardness of cryolite

Previous studies have shown cryolite is a hygroscopic material subject to degradation if not kept in a relatively dry environment or hermetically sealed in the coating design [10]. To prevent the degradation and preserve the spectral efficiency of the deposited cryolite overcoat, we investigated two respective methods; the cryolite was deposited using reactive physical vapor deposition (rPVD) in a background of low vapor pressure xenon di-fluoride (XeF_2), and a thin overcoat of MgF_2 (i.e., ~3 nm) was deposited on the overcoat of cryolite ex-situ using atomic layer deposition (ALD).

The rPVD process is utilized to passivate the aluminum and create a thin layer of aluminum tri-fluoride (AlF_3) prior to depositing the metal fluoride using PVD. It also aims to fill in voids and increase the fluorine efficiency of the deposited metal fluoride coating similar to the rPVD processes as used with other refractive oxide films [11-13]. Furthermore, we have shown in prior research this process improves the environmental durability of PVD deposited lithium fluoride (LiF) [14]. The process outlined in Section 2.1 was utilized, however, 1.7 sccm of XeF_2 gas was inserted into the coatings chamber immediately following the deposition of the aluminum. The chamber was then further evacuated and the cryolite was deposited at a working pressure of $\sim 3x10^{-7}$ torr. As the final step, residual XeF_2 in the precursor gas lines was inserted into the chamber at pressures up to $5x10^{-4}$ torr to further passivate the coating.

We collaborated with the Jet Propulsion Laboratory (JPL) to grow MgF_2 using ALD [4]. The process creates a thin homogeneous protective barrier over the cryolite in the order of a few monolayers to sufficiently protect the material from degradation. The MgF_2 was deposited using bis-(ethylcyclopentadienyl) magnesium and anhydrous fluoride (HF) precursors at 100°C substrate temperatures. Five ALD cycles of 750 ms and 60 ms exposure were utilized for the respective magnesium precursor and hydrofluoric acid (HF). Exposures were kept at a continuous 80 sccm purge flow of Argon with a purge time of 2 minutes and 4 minutes for the respective magnesium precursor and HF steps. The working pressure for the process was ~380 mTorr with MgF_2 growth rates up to 0.5 Å/sec.

2.3 Surface and spectral characterization

The surface properties of the films were measured using the NanoCam© optical profilometer with a 20X Linnik interference objective, and the PARK AFM NX20© atomic force microscope (AFM) shown in Figure 1. The instruments were selected to cover the nanometer to millimeter spatial waviness of the samples. This will allow us to determine the bandlimited surface roughness properties of the deposited films as we will analyze film morphology as well as sample scatter due to irregularities in the film deposition process or aging of the films. Based on the pixel size, magnification, and resolution of the instruments, the Nanocam© covers the ~1-400 μm level spatial irregularity waviness while the scanning parameters of the Park AFM NX20© were set to cover spatial waviness from ~.02-8 μm. The AFM was operated at contact mode with a 0.5 Hz scan rate. The Power Spectral Density (PSD) was analyzed for the surface maps as performed in previous publications [15].

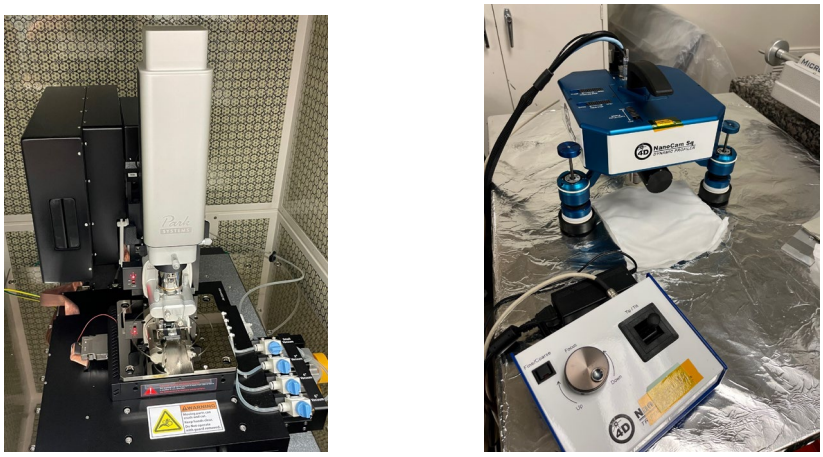

a. b.

Figure 1. Surface roughness characterization instruments including the a) inside of Park AFM NX20© displaying the measurement head and automated x and y sample stage and b) Nanocam© profilometer with motor-driven focus and tip/tilt adjustment.

The sample reflectance was measured using the McPherson vacuum ultraviolet (VUV) 225 spectrometer. The spectrometer contains a windowless gas-purged source compatible with various gases to analyze the 30 nm to 325 nm spectral band. The primary gas source used in our setup was hydrogen as it provides a pseudo continuum at wavelengths ranging from 90 nm to the visible spectrum. The unit is equipped with a meter-long monochromator with an interchangeable 1200 line/mm toroidal grating which serves as both the dispersive and imaging element as it not only separates the spectra of the gas, but it images the entrance slit into the exit slit. The detector utilized is a photomultiplier tube (PMT) equipped with a scintillator to fluoresce the FUV light into the visible. Absolute reflectance measurements were performed by measuring the incident beam both without and with the optic in the optical path. Reflectance measurements were performed at 10° angle of incidence.

The UV to infrared reflectance, dispersive properties, and thickness of the deposited film were measured utilizing the HORIBA scientific UVISEL Plus spectroscopic ellipsometer© and the Perkin Elmer PE950© spectrometer. The PE950© covers a measurement range of 200-3000 nm using interchangeable sources and detectors providing absolute spectral measurements. The ellipsometer has a measurement range of 190-2100 nm and is equipped with a polarizer and analyzer for measurement and analysis of the ellipsometry terms Ψ and Δ. Once these ellipsometry terms are known, the thickness and refractive index of the deposited dielectric film is derived from the experimental data using the Lorentz oscillator model.

2.4 Environmental aging tests

Extensive research has been performed on deposited metal fluorides and their hygroscopic and/or hydrophilic nature [16-18], thus, the samples in these experiments were exposed to temperature and relative humidity (RH) conditions to examine the samples degradation properties. The samples were kept in ambient lab environments with temperature ranging from 22-24°C and RH levels of 50-60%.

3. RESULTS AND DISCUSSION

3.1 Spectral efficiency performance and aging

Several Al-cryolite samples were produced using conventional PVD while ALD and rPVD methods were implemented to assess the effectiveness of these methods to protect the cryolite from degradation. These processes are described in Sections 2.1 and 2.2 while select deposition parameters for the samples in this study are shown in Table 1. Samples AC1-AC5 were produced using conventional PVD processes, however, sample AC5 was overcoated with a 3 nm layer of MgF_2 using an ex-situ ALD process. Sample AC6 was produced using the rPVD process.

Table 1. Parameters of produced samples of Al with an overcoat of cryolite.

Sample ID	Al/Na_3AlF_6 thickness (nm)	Max Substrate temperature* (°C)	Deposition Process of cryolite	Aging (days)
AC1	65/26	24	PVD	Stored
AC2	65/24	24	PVD	Stored
AC3	65/26	24	PVD	Stored
AC4	65/26	24	PVD	112
AC5	65/26	100	PVD + ex-situ ALD MgF_2	75^+
AC6	65/23	24	rPVD	90

*Substrate temperatures based on activation energy added to process (i.e., heating of substrate prior to deposition). Substrate temperature changes due to kinetic energy of deposited material or heat transfer from condensed deposited material onto substrate not considered.

+Sample AC5 was aged 29 days prior to ALD MgF_2 application then an additional 75 days

The FUV spectral reflectance performance is shown in Figure 2. All samples excluding sample AC2 were optimized for high reflectance at wavelengths >120 nm, thus, samples AC1 and AC3-AC6 produced an average spectral reflectance of 90-93% at the 120-170 nm FUV spectral band while resulting in 93-96% reflectance at the HLyα spectral line. Sample AC2 was optimized for wavelengths <120 nm as a thinner cryolite layer was deposited on Al; this resulted in an average reflectance of ~88% in the 120-180 nm band and 91% reflectance at the HLyα spectral line. It is noteworthy that all PVD processes were performed at ambient chamber conditions with no activation energy applied. Typically, optics coated with metal fluorides are heated to 250-270°C during or post-deposition of the respective metal fluoride material or the metal fluoride is deposited at high rates to optimize its crystalline structure. [19]; as cryolite is deposited using conventional methods, irregularities which may arrives from respective processes such as heating non-uniformities due to optic size and coating artifacts which may cause scatter are mitigated. The only sample not kept at ambient temperature throughout its entire manufacturing process is AC6 which was heated to 100°C after the PVD process to apply ALD MgF_2.

Furthermore, it is shown the Al + cryolite samples produced using methods for enhanced durability did not impact the spectral performance compared to conventionally deposited samples. The spectral reflectance of the samples which were processed for enhanced durability (i.e., ALD MgF_2 overcoat and rPVD), AC5 and AC6, performed equivalent to the conventionally deposited samples as the respective reflectance at the HLyα spectral line was 94% and 96% with an average reflectance of 90% and 91% over the 120-170 nm spectral band. This is in line with the average spectral performance of the produced cryolite samples.

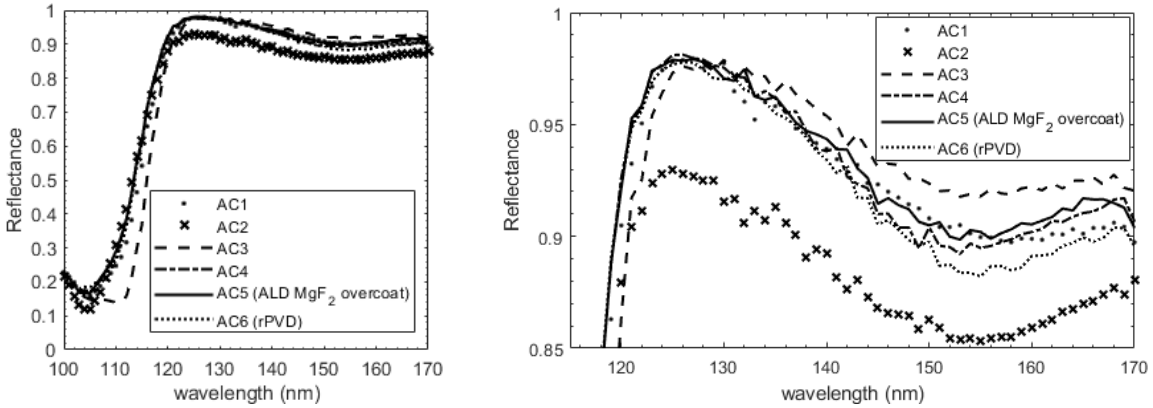

Figure 2. Spectral reflectance of Al+cryolite test samples measured immediately following the deposition processes. The same substrate material and respective mechanical dimensions were used for all tests. Sample AC2 contained a thinner cryolite. Nearly all samples obtained a spectral reflectance of >94% at 121.6 nm as the only sample not achieving this, AC2, contained a thinner metal-fluoride overcoat thickness.

FUV spectral reflectance performance is compared as the samples were aged 75-122 days as summarized in Table 1. As displayed in Figure 3, the reflectance over the 120-170 nm spectral band remained the same for all samples after aging as the slight variations are within the measurement error of the instrument. Even sample AC3 which had no environmental hardness processes applied, irregularities arising as the cryolite coating aged did not cause significant change in the effective index of the material. Previous research of cryolite multilayer films has observed changes in the in effective index of these films as irregularities form and expand over the measured aperture [10]. During the period of this research, irregularities arising during aging did not cause significant change to affect the spectral properties of the film as the size and frequency of irregularities had no impact over the integrated diameter of the spectrometer beam during measurement.

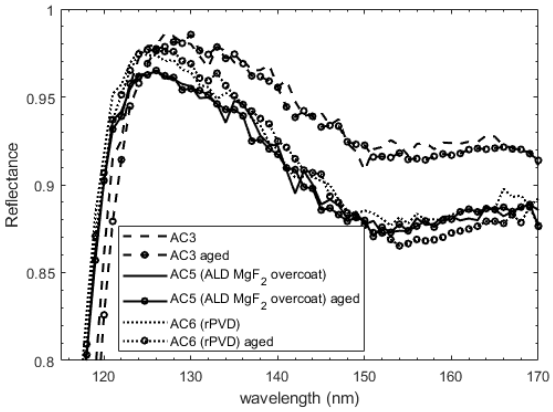

Figure 3. FUV spectral reflectance of Al + cryolite test samples. There were no significant spectral reflectance changes after aging.

The average reflectance and index of refraction of samples AC3, AC5, and AC6 in the ultraviolet to infrared spectral region are respectively shown Figure 4a and 4b. The average reflectance at this spectral range is in line with conventional metal fluoride protected aluminum samples with reflectance >85% in the UV to visible and ~85%-97% in the near-infrared (NIR) to short-wave infrared (SWIR) [1]. The index of refraction of the deposited cryolite films is also slightly higher than that reported by literature as indices of refraction from 1.3-1.34 have been previously reported in for the thin film coating and the bulk material [8,20]. This suggests a higher packing density for our produced cryolite films. Furthermore, ellipsometry measurements showed a slightly higher index of refraction for the rPVD deposited film (AC6) compared to the conventionally deposited film (AC3). Although the difference is within the measurement error of the instrument, this suggests that the cryolite film in sample AC6 is denser with less voids compared to that in AC5.

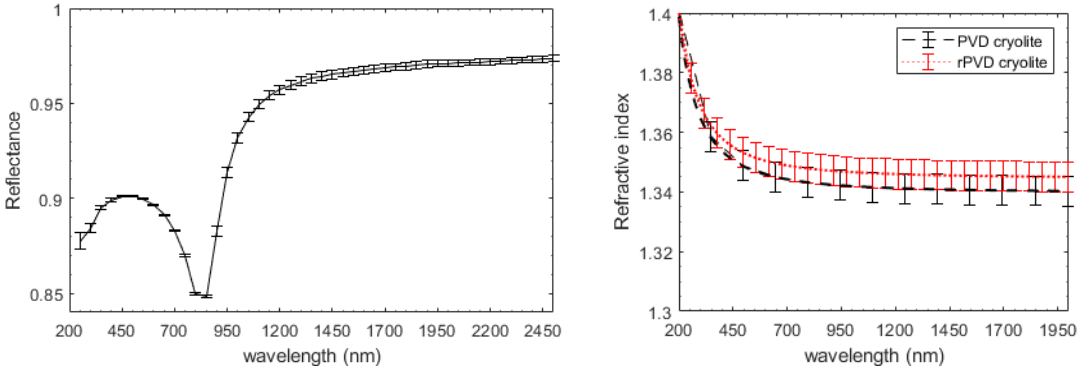

a. b.

Figure 4. a) Average reflectance of Al + cryolite samples with error bars displaying ±standard deviation of all samples measured and b) measured refractive index of samples AC5 and AC6 immediately after deposition in the ultraviolet to infrared.

3.2 High spatial frequency surface irregularities and surface defects

The surface roughness and defects are compared for samples AC3, AC5, and AC6 after aging as specified in Table 1. As shown in Figure 5b, sample AC3 develops the worst degradation after aging as a substantial amount of pore shaped voids are formed and the RMS surface roughness increased from 0.4 nm to 0.6 nm per ~0.5 x 0.4 mm^2 area. Although the mean pore diameter per unit area remained consistent, the standard deviation of the pore diameter increased by a factor of 5, indicating an increased average pore area dispersion. The maximum measured pore diameter increased from 74 µm to 110 µm for this sample. This indicates the addition of detected pores with previous pores increasing in size for sample AC3. These results are consistent with previous research of cryolite multilayer coatings as pore formation and pore diameter increase was observed as samples were aged due to capillary condensation as the voids/pores become filled with water [10]. The quantity and size of the pores is smaller for our coating application compared to these published results.

These pore shaped voids are less apparent in samples AC5 and AC6. Although there are visible pores on samples AC5, the pore quantity per unit area, the mean pore diameter, and the max pore diameter showed no significant change, indicating that these defects may have formed before applying the ex-situ ALD overcoat as this overcoat significantly slowed degradation. Sample AC6 showed the least visible and measured degradation, as no significantly sized pores were detected and the RMS roughness over the measured area did not change. The mean and max pore diameter remained the smallest for samples AC6 as there were very little defects with the maximum pore diameter observed over the total aging period was 9 µm. The results are summarized in Table 2 for all samples. This confirms the effectiveness of the enhanced durability processes as there are substantially fewer voids/pores on these samples compared to sample AC3.

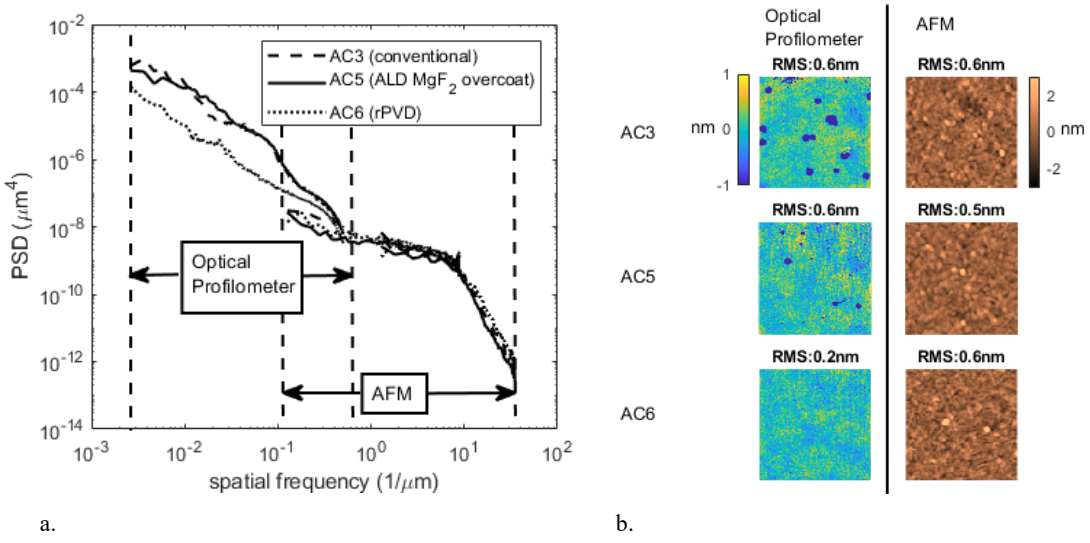

Figure 5. a) Power Spectral Density (PSD) and b) surface roughness maps of Al+cryolite samples conventionally deposited (AC3), capped with an MgF_2 overcoat layer (AC5), and deposited using rPVD (AC6) after respective aging indicated on Table 1. Exemplary measured surface maps over a 512 µm x 442 µm area as measured by the Nanocam© optical profilometer and a1 µm x 1 µm area as measured by the AFM NX20© are shown. Sample AC6 performed the best as the coating degraded the scatter properties of the film minimally.

As the surface defects and roughness of the films are isotropic and homogeneous, the radially averaged surface power spectral density was analyzed to observe the dominant spatial frequencies affected by the degradation as well as impacts of the degraded surface on the scatter properties of the film. As seen in the surface roughness maps of Figure 5b, the conventionally deposited samples (AC3) contain the most visible degradation followed by the samples with the ALD MgF_2 overcoat (AC5). The rPVD (AC6) sample shows no visible degradation. The PSD also shows degradation at spatial frequencies lower than ~0.1 μm^{-1}, corresponding to ~100 µm surface irregularity periods for the AC3 and AC5 compared to the rPVD (AC6) sample; this is due to the periodic voids which were formed on the AC3 and AC5 samples due to degradation.

The surface roughness in the coating morphology spatial frequency range of ~100-1 μm^{-1}-as measured by the AFM remained the same for all Al+cryolite coated samples. Regardless of the surface voids which were formed on the AC3 sample, the roughness distribution was identical to samples AC5 and AC6 at this spatial irregularity range if not measured at the pore-forming areas. This indicates that for sample AC3, periodic pore formation for this aging period is beyond the nm surface spatial waviness which would impact the spectral performance in the FUV; however, these pores will cause scatter/stray light effects in the larger spectral bands while their dynamic behavior and chemical stability over large periods of time are unknown. Samples AC5 and AC6 showed better stability with few to no pores formed on the surface, thus, scattering will be less of a concern for these samples.

Table 2. Surface irregularities including pore formation and roughness of samples AC3, AC5, and AC6 during aging.

Sample	Aging temperature (°C)/relative humidity %	Aging (days)	Average RMS surface roughness over 512x442 μm^2 area	Average # of pores per 512 x 442 μm^2 area/mean diameter/ max diameter/ area covered	Aging (days)	Average RMS surface roughness over 512x442 μm^2 area	Average # of pores per 512 x 442 μm^2 area/mean diameter/ max diameter/ area covered
AC3	22-24/50-60	72	.4 nm	7±3 / 66±5 µm / 74 µm / 2.3%	112	.6 nm	11±5 / 65± 20 µm / 110 µm / 4.3%
AC5	22-24/50-60	35	.3 nm	8±3 / 39±10 µm / 57 µm / 1.0%	75	.6 nm	9±3 / 37± 12 µm / 60 µm / 1.3%
AC6	22-24/50-60	50	.3 nm	n/a	90	.2 nm	3±2 / 7±1 µm / 9 µm / 0.02%

4. CONCLUSION

We have demonstrated the production of high spectral efficiency broadband FUV reflectors consisting of Al overcoated with cryolite for use in FUV spectroscopy. These reflectors yielded a spectral reflectance of 93-96% in the HLyα spectral line with an average of 90-93% in the 120-170 nm spectral band, while performing nominal to protected aluminum coatings in the UV-SWIR. The spectral efficiency of the reflectors shows little change as they were aged 75-112 days in a relatively high humidity environment.

We have also demonstrated novel methods to improve the environmental hardness of cryolite overcoat coatings over aluminum. By adding a hermetic layer of a few monolayers of MgF_2 using ALD over the Al + cryolite coating, the degradation of the cryolite coating was halted as the voids on the coating did not grow in frequency or size during the aging period. Additionally, a novel reactive evaporation method was introduced which prevented void formation and produced the most environmentally cryolite coating material with minimal observed irregularities while retaining its RMS surface roughness.

5. ACKNOWLEDGEMENTS

We acknowledge SAT proposal grant 21-SAT21-0027 which supported part of this effort. We also acknowledge the NASA JPL facilities for supporting the ALD tasks in this effort. LRM acknowledges the support of CRESST II cooperative agreement, which is supported by NASA under award number 80GSFC21M0002.

REFERENCES

[1] Manuel A. Quijada, Javier Del Hoyo, Stephen Rice, "Enhanced far-ultraviolet reflectance of MgF2 and LiF over-coated Al mirrors," Proc. SPIE 9144, Space Telescopes and Instrumentation 2014: Ultraviolet to Gamma Ray, 91444G (24 July 2014); https://doi.org/10.1117/12.2057438

[2] Keski-Kuha, Ritva & Larruquert, Juan & Gum, J. & Fleetwood, C. (1999). Optical Coatings and Materials for Ultraviolet Space Applications. 164. 406.
[3] Manuel A. Quijada, Javier G. Del Hoyo, Emrold Gray, J. Gabriel Richardson, Andrew Howe, Luis Rodriguez de Marcos, David A. Sheikh, "Influence of evaporation rate and chamber pressure on the FUV reflectance and physical characteristics of aluminum films," Proc. SPIE 11819, UV/Optical/IR Space Telescopes and Instruments: Innovative Technologies and Concepts X, 118190G (20 August 2021); https://doi.org/10.1117/12.2595392.
[4] John Hennessy, April D. Jewell, Frank Greer, Michael C. Lee, Shouleh Nikzad; Atomic layer deposition of magnesium fluoride via bis(ethylcyclopentadienyl)magnesium and anhydrous hydrogen fluoride. *Journal of Vacuum Science & Technology A* 1 January 2015; 33 (1): 01A125. https://doi.org/10.1116/1.4901808 Jones, C. J., Director, Miscellaneous Optics Corporation, interview, Sept. 23 2011
[5] I. Barrett, J. Herron, T. Rahmlow, and R. L. Johnson, "Cryolite – a new look at an old standby," in *Optical Interference Coatings 2016*, OSA Technical Digest (online) (Optica Publishing Group, 2016), paper TB.4.
[6] Mao, Shuzheng, and Jianzheng Xi. "Thin film beamsplitters." *Second International Conference on Thin Film Physics and Applications*. Vol. 2364. SPIE, 1994.
[7] RING, J., WILCOCK, W. Multilayer Dielectric Reflecting Films at Wave-lengths between 4000 and 4600 A.. *Nature* **173**, 994 (1954). https://doi.org/10.1038/173994a0
[8] R. P. Netterfield, "Refractive indices of zinc sulfide and cryolite in multilayer stacks," Appl. Opt. 15, 1969-1973 (1976)
[9] Fabricius, Henrik. "Developments in the design and production of error-sensitive smart coatings." *Developments in Optical Component Coatings*. Vol. 2776. SPIE, 1996.
[10] Borucki, William J., ed. *Second Workshop on Improvements to Photometry*. Vol. 10015. NASA Ames Research Center, Chapter 4, pg. 307-316 (1988).
[11] Cosnier, M. Olivier, G. Théret, B. André; HfO2–SiO2 interface in PVD coatings. *Journal of Vacuum Science & Technology A* 1 September 2001; 19 (5): 2267–2271.
[12] Maiti, Namita, et al. "Effects of oxygen flow rate on microstructure and optical properties of aluminum oxide films deposited by electron beam evaporation technique." *Vacuum* 85.2 (2010): 214-220.
[13] Ferrieu, E., and B. Pruniaux. "Preliminary investigations of reactively evaporated aluminum oxide films on silicon." *Journal of The Electrochemical Society* 116.7 (1969): 1008.
[14] Quijada, Manuel A., et al. "Advanced Al mirrors protected with LiF overcoat to realize stable mirror coatings for astronomical telescopes." *Advances in Optical and Mechanical Technologies for Telescopes and Instrumentation V*. Vol. 12188. SPIE, 2022.
[15] Del Hoyo, Javier, et al. "Experimental power spectral density analysis for mid-to high-spatial frequency surface error control." *Applied optics* 56.18 (2017): 5258-5267.
[16] Fleming, Brian, et al. "Advanced environmentally resistant lithium fluoride mirror coatings for the next generation of broadband space observatories." *Applied Optics* 56.36 (2017): 9941-9950.
[17] Lewis, Devin M., et al. "Illuminating the degradation of lithium fluoride mirror coatings in humid environments." *Advances in Optical and Mechanical Technologies for Telescopes and Instrumentation IV*. Vol. 11451. SPIE, 2020.
[18] Punwani, Dharamvir, C. W. Chi, and D. T. Wasan. "Dynamic Sorption by Hygroscopic Salts. A Comparative Study." *Industrial & Engineering Chemistry Process Design and Development* 7.3 (1968): 410-415.
[19] L. Rodríguez-de Marcos, B. Fleming, J. Hennessy, D. Chafetz, J. Del Hoyo, M. Quijada, M. Bowen, D. Vorobiev, B. Indahl, "Advanced Al/eLiF mirrors for the SPRITE CubeSat," Proc. SPIE 12188, Advances in Optical and Mechanical Technologies for Telescopes and Instrumentation V, 1218820 (29 August 2022); https://doi.org/10.1117/12.2630522
[20] Pauly, H.. (1977). Cryolite, chiolite and cryolithionite: optical data redetermined. Bulletin of the Geological Society of Denmark. 26. 95-101. 10.37570/bgsd-1976-26-07.